Indian Journal of Pure & Applied Physics
Vol. 62, May 2024, pp. 339-349
DOI: 10.56042/ijpap.v62i5.7952

Revisiting Some Pismis Open Clusters Using Gaia Environmental Technology

Amjad A Al-Subaie & Amnah S Al-Johani*
Mathematics Department, Faculty of Science, University of Tabuk 47512, Saudi Arabia

Received 10 January 2024; accepted 5 February 2024

In this study, we considered the collective members of Pismis's clusters located at identical distances r(pc) and distributed around a mean absolute magnitude (M_o) following a Gaussian distribution with dispersion (σ). We computed the distances r_c(pc) of these clusters by applying a distance equation designed to account for Malmquist bias. Our computed distances were in satisfactory agreement ($\sim 99\%$) when compared to previous research findings.

In the second part of our work, we delved extensively into the Pismis 3 cluster, which is rarely studied, aged, and among the most affluent. We conducted analyses on its dynamical tidal radius ($x_L = r_t = 14.60 \pm 1.26$ pc), crossing time ($T_{cross} = 1.363 \pm 0.014$ Myr), relaxation time ($T_{relax} = 11.56 \pm 3.40$ Myr), and angular velocity ($\Omega_o = 0.024 \pm 0.001$km s^{-1}).

A kinematic analysis of these open clusters was carried out, encompassing aspects such as their apex position (A_o, D_o) using the AD chart method, velocity ellipsoid parameters (VEPs), and the longitude of the vertex (l_2) revealing a minimal value, as anticipated when pointing exactly at the Galactic Center. Additionally, we explored their ages in relation to evolution, linking them to formation mechanisms, metallicity, and opacity.

Keywords: Statistical methods; Open clusters and associations; Pismis open clusters; Distance equation; Kinematics and dynamics; Longitude of the vertex (l_2).

1 Introduction

Open clusters (OCs) serve as excellent indicators for discerning the spiral arm structure and evolution of the Galactic disc[1–6]. They provide a valuable means to test stellar and dynamical evolution[7–11], enabling exploration of star creation mechanisms and their recent history. Additionally, OCs play a crucial role in constraining the initial luminosity and mass functions (LF and IMF) within groups of stars.

Moreover, the radial velocities of OCs have proven instrumental in tracing local kinematics, including Solar motion, Oort's constant A, and the rotation curve.

Clusters with ancient origins, situated at considerable distances, play a crucial role in establishing disk abundance gradients. The correlation between cluster age and metallicity indicates an intricate history of chemical enrichment and mixing within the disk[4].

Considering the factors mentioned above, we identify Pismis open clusters by utilizing Schmidt plates. The astronomer from the late fifties[12] who compiled a catalog of 24 open and 2 globular clusters in the Southern Milky Way along the Galactic plane ($225^o \geq l \geq 353^o$)is referenced. The catalog covers clusters with ages ranging from 6.86 to 9.40 (log yr^{-1})[13]. Based on the Galactic longitude (l)and log (age) of Pismis (hereafter Pis), we focused on18clusters (*i.e.*, Pis 1 to Pis 5, Pis 7, Pis 8, Pis 11, Pis 12, and Pis 15 to Pis 23). The data for these clusters were obtained from Gaia DR3[1] open clusters in the Milky Way[14], the Gaia mission collaborations data release 3 has been used to get the astrometric data. A new chapter in Astronomy has begun since the launch of the European Space Agency (ESA) mission Gaia as it contains the five-parameter astrometry for approximately 1.8 billion sources along their position in the sky (α, δ), parallaxes (π; mas) and the right ascension and declination components of the proper motion ($\mu_\alpha \cos\delta, \mu_\delta$; mas yr^{-1}) with limiting magnitude of G = 21 mag. With uncertainties in the respective proper motion, components are up to 0.02 – 0.03 mas yr^{-1} (at G < 15 mag), 0.07 mas yr^{-1} (at G ~ 17 mag), 0.50 mas yr^{-1} (at G ~ 20 mag) and 1.40 mas yr^{-1} (at G = 21). The uncertainties in the parallax values are ~ 0.02 – 0.03 mas for sources with G < 15 mag, ~ 0.07 mas for sources with G = 17 mag, ~ 0.50 mas at G = 20 mag, and ~ 1.30 mas at G = 21. The DR3 is complemented with data of the radial velocity (V_r; km s^{-1}) for about 7 million stars from DR2[16]. The source list has a slight change to DR2

*Corresponding author: (E-mail: aalgohani@ut.edu.sa)

with some notable changes. The significant advance of DR3 over DR2 is the large improvement in the accuracy of the astrometric parameters; a factor of 2.00 in proper motion accuracy and a factor of about 1.50 in the parallax accuracy. Astrometric errors were suppressed by 30 – 40% for the parallax and by a factor of 2.50 for the proper motion. In our calculations, we consider members with a probability ($P \geq 50\%$) based on Gaia DR3[1].Due to the absence of radial velocity data, we supplement it with information from other sources, as elaborated later.

Our article aims to use the distance equation to compute the distances of Pis clusters depending on the so-called Malmquist bias. We also seek to determine various dynamical and kinematical structures, including relaxation time (T_{relax}; Myr), evolving time (τ_{ev}; Myr), apexes (A_o, D_o) using the AD chart method, and the longitude of the vertex (l_2; deg).

The structureof the present work is organized into three main sections. First,we introduce the target clusters and their fundamental parameters obtained through Gaia DR3[1], as described in Section 2. The next section encompasses the results and discussion, delving into astrometric and dynamical parameters, as well as the kinematical structure, as outlined in Section3. Finally, we conclude our findings in Section4.

2 Target Clusters and Their Fundamental Parameters

As previously mentioned, Pisclusters were investigated using Schmidt plates at the Tonanzintla observatory[12]. In Table 1, we have compiled information for 18Pis clusters (Pis 1 to Pis 5, Pis 7, Pis 8, Pis 11, Pis 12, and Pis 15 to Pis 23) with a membership probability ($P \geq 50\%$) designating the mas higher probable candidates[14]. In instances where radial velocity data (V_r) were unavailable, we supplemented the information with another source[17]. A brief history and characteristics of Pis clusters are given below:

- Pis 1: This small open cluster exhibits a diameter of 3 arcmin. It is situated2000 pc from the Sun and30 pc from the Galactic plane. With an age of approximately 9×10^7yr, it falls under Trupmler classification class I3p[18].
- Pis 2: Described as a poorly studied open cluster with an intermediate age, Pis 2 is located toward the outerpart of our Galaxy within a highly reddened Galactic zone[19]. It is likely positioned inside a dust layer[20], with an estimated age ranging from 1.1 to 1.2 Gyr.
- Pis 3: This cluster, rarely studied, was examined by Tadross[21]. The study aimed to re-determine its physical parameters using photometric and astrometric analysis with 2MASS[22]. The findings include a metallicity (Z) of 0.008 and an estimated age of 2.24 Gyr.
- Pis 4: Also known as C 0832-441, Pis 4 recently made an appearance in the open cluster multi-membership catalog[23]. Positioned at 593 pc, it exhibits a reddening value [E (B–V)] of 0.01. The age (log yr^{-1}) is approximately 7.53.
- Pis 5: Referred to as ESO 313-SC7, Pis 5 is a young and low-mass cluster located in Vela. Its field features a small number of bright stars

Table 1 — Fundamental parameters of Pis clusters ($P \geq 50\%$) according to Gaia[17]

Clusters[a]	Alternative name[b]	Members[14] (N)	Ra. (2000)[14] h m s	Dec. (2000)[14] d m s	l[14] deg.	b[14] deg.	$(\mu_\alpha \pm \sigma_\alpha)$[14] mas yr^{-1}	$(\mu_\delta \pm \sigma_{\mu\delta})$[14] mas yr^{-1}	$(\pi \pm \sigma_\pi)$[14] mas	$(V_r \pm \sigma_{Vr})$[17] km s^{-1}	Age[13] log yr^{-1}
Pis 1	C 0815-369	84	08 18 19.20	–37 06 07.2	255.116	–0.709	–2.611 ± 0.014	3.966 ± 0.013	0.145 ± 0.005	-	7.928
Pis 2	C 0816-414	208	08 17 54.48	–41 40 26.4	258.858	–3.341	–4.756 ± 0.016	5.325 ± 0.018	0.221 ± 0.007	58.99 ± 1.69	9.060
Pis 3	C 0829-385	1083	08 31 20.16	–38 38 24.0	257.853	0.503	–4.809 ± 0.005	6.645 ± 0.006	0.403 ± 0.002	30.33 ± 0.25	9.027
Pis 4	C 0832-441	122	08 35 09.60	–44 24 25.2	262.916	–2.353	–8.236 ± 0.021	5.337 ± 0.018	1.414 ± 0.004	11.59 ± 3.55	7.533
Pis 5	ESO 313-7	102	08 37 37.68	–39 36 10.8	259.355	0.905	–5.494 ± 0.025	4.275 ± 0.026	1.026 ± 0.008	-	7.197
Pis 7	C 0839-385	131	08 41 08.88	–38 41 56.4	259.053	1.997	–3.312 ± 0.01	2.793 ± 0.013	0.15 ± 0.005	74.40 ± 1.04	8.700
Pis 8	C 0839-461	59	08 41 37.68	–46 16 19.2	265.089	–2.578	–5.757 ± 0.019	4.945 ± 0.014	0.517 ± 0.007	-	7.427
Pis 11	HD 80077 Group	49	09 15 53.76	–50 00 21.6	271.65	–0.699	–5.397 ± 0.015	3.926 ± 0.02	0.335 ± 0.009	-	7.000
Pis 12	ESO 261-5	217	09 20 01.68	–45 07 51.6	268.653	3.21	–6.748 ± 0.013	4.833 ± 0.01	0.431 ± 0.004	32.44 ± 0.50	9.400
Pis 15	C 0932-479	150	09 34 44.16	–48 02 24.0	272.495	2.863	–5.302 ± 0.01	3.329 ± 0.011	0.354 ± 0.004	36.28 ± 0.68	9.110
Pis 16	C 0949-529	10	09 51 14.88	–53 10 19.2	277.83	0.683	–5.794 ± 0.03	3.471 ± 0.021	0.356 ± 0.007	21.00 ± 9.00	7.839
Pis 17	Cl Pismis 17	51	11 01 30.48	–59 52 22.8	289.539	0.109	–6.938 ± 0.017	2.333 ± 0.015	0.366 ± 0.005	–44.60 ± 5.20	7.023
Pis 18	Cl Pismis 18	291	13 36 54.48	–62 05 27.6	308.226	0.313	–5.658 ± 0.007	–2.286 ± 0.008	0.332 ± 0.004	–28.45 ± 0.63	9.080
Pis 19	Cl Pismis 19	472	14 30 39.84	–60 53 20.4	314.71	–0.307	–5.46 ± 0.007	–3.247 ± 0.011	0.255 ± 0.004	–29.55 ± 0.30	8.900
Pis 20	Cl Pismis 20	149	15 15 23.52	–59 04 22.8	320.514	–1.206	–3.831 ± 0.013	–2.911 ± 0.012	0.291 ± 0.005	–76.71 ± 1.01	6.864
Pis 21	HD 135159 Group	135	15 16 47.76	–59 39 32.4	320.358	–1.799	–4.143 ± 0.011	–3.761 ± 0.012	0.29 ± 0.005	-	8.110
Pis 22	Cl Pismis 22	88	16 14 12.48	–51 52 08.4	331.473	–0.605	–3.882 ± 0.025	–4.263 ± 0.017	0.102 ± 0.012	–52.58 ± 0.42	7.600
Pis 23	Cl Pismis 23	87	16 23 57.60	–48 53 27.6	334.668	0.431	–2.679 ± 0.038	–3.209 ± 0.029	0.166 ± 0.017	-	8.480

(a)[14], (b)[12], (c)[17], and (d)[13].

mixed with gas emissions and dust. The single work on Pis 5 involved UBV+ H_β photometric analysis[2], where it was not initially considered a star cluster. Bonatto and Bica[24] later derived astrophysical parameters, revealing a poorly populated main sequence with near-infrared reddening [E (J–H) = 0.13 ± 0.01]. The corresponding values include E (B–V) = 0.42 ± 0.03 or A_V = 1.3 ± 0.1, and the distance from | the Sun is 1.0 ± 0.1 kpc.

- Pis 7: This cluster is described as small and faint, with an apparent diameter of about 3 arcmin, belongs to Trumpler class II1m[25]. Extensive analysis suggests an age (log yr^{-1}) of approximately 8.70, and the cluster is situated at 4.9± 1.3 kpc. Interestingly, the cluster appearsto be around 200 pc below the Galactic plane andapproximately10–11 kpc from the Galactic Center[26].
- Pis 8: Identified as a poorly studied open cluster, Pis 8 is located along the axis of the local area when observed from the Sun in the Vela-Pup pis (extending from 240° to 280° in Galactic longitude) regions of our Galaxy. Its age is estimated to be about 5–7 Myr, and it is positioned at 2000 pc from the Sun[27].
- Pis 11: The cluster underwent a global study[28], revealing the presence of a single O-type star and some early B-type stars. The cluster is situated at approximately 3.6 kpc, and in the vicinity of the cluster, there are several early-type stars at the same distance.
- Pis 12: Pis 12 appears to contain only a random mixture of red stars, suggesting the absence of a distinct cluster star[29]. However, it has also been considered as a star cluster in another study[30].
- Pis 15: This cluster seems to be populated by stars with magnitudes in the range of $22 \geq M_V \geq 14$. It rises above the background, with a radius no larger than 1.8 arcmins. The estimated age of Pis 15 is about 1.3 Gyr[31].
- Pis 16: known as C 0949-529, Pis 16 is identified as a young open cluster with proper motion in both directions:−15.1 and7.4 (mas yr^{-1})[32].
- Pis 17: Described as a compact cluster with an E (B–V) value of 0.51 ± 0.07 and about 4.2 kpc[29].
- Pis 18: Described as a moderately populated and intermediate-age open cluster, Pis 18 is situated around the inner disc (R_{GC}< 8 kpc) and is found inside the Solar circle at a Galactocentric separation of approximately 7 kpc. The estimated age is 700^{+40}_{-50} Myr, with E (B–V) of $0.562^{+0.012}_{-0.026}$ mag. It also possesses a radial velocity of about −27.5 ± 2.5 (km s^{-1})[33].
- Pis 19: Described as a compact and intermediate-age open cluster, Pis 19 had its fundamental parameters updated by Carraro and Munari[34]using CCD multicolor photometry. It has an estimated age of~800 Myr, E (B–V) of 1.48 ± 0.15, and a distance onthe order of 1.4 ± 0.4 kpc from the Sun.
- Pis 20: Avery young cluster with an age of 5 Myr, Pis 20 is a concentrated group of stars composed of two superimposed groups along the line of sight. It has a diameter of about 2 arcmins and is in the Norma-Scutum (-II) arm of the Galaxy[35].
- Pis 21: Identified as a poorly studied open cluster, Pis 21 is positioned near the central part of our Galaxy. It lacks a clear main sequence or other distinctive features. The cluster was observed using a color-magnitude diagram (CMD)[36] with CCD in BVI pass bands, reaching down to M_V~ 19 mag.
- Pis 22: Situated toward the central parts of the Galaxy, Pis 22 is located close to and in the field of the small emission nebula RCW103 (G332.4-0.4, PKS 1613-50). This nebula is presently identified as a supernova remnant at an estimated distance of 6.6 kpc[37,38]. CCD observations[36] in the BVI passbands were conducted for stars in the fields of this open cluster, adopting E (B–V) = 2.00 ± 0.10 mag, an age of ~40 ± 15 Myr, and a distance of 1.0± 0.4 kpc.
- Pis 23: Also known as Lynga 10[39], BH 190[40], or ESO226-SC5[41], Pis 23 is located beyond the Sagittarius arm and stands among the foremost blushed and distant open clusters known within the direction toward the Galactic Center. Claria and Piatti[42] determined its reddening [E (B–V)] to be 2.0 ± 0.1, the distance from the Sun to be ~2.6 ± 0.6 kpc, and an age of almost 300 ± 100 Myr.

Table 1 presents the fundamental parameters of Pis clusters from sources[14], Pismis[12], and open cluster kinematics[17], arranged as follows:

Columns 1 and 2: Cluster name and alternative name

Column 3: Number of members (N)

Columns 4 and 5: Coordinate elements, *i.e.*, right ascension and declination (degrees)

Columns 6 and 7: Coordinate elements, *i.e.*, Galactic longitude and Galactic latitude (degrees)

Column 8: Proper motion along right ascension with uncertainties (mas yr^{-1})

Column 9: Proper motion along with declination with uncertainties (mas yr^{-1})

Column 10: Parallax and uncertainties (mas)

Column 11: Available radial velocity and uncertainties (km s^{-1})

Column 12: Age (log)

3 Results and Discussion

3.1 Astrometric Parameters

Interstellar extinction, involving both components (absorption and scattering), influences distance determination, not solely the absorption component. While the absorption component may dominate in regions abundant with gas and dust, scattering caused by duct is also significant. One of the challenges in studying Galactic star clusters lies in distance determination, requiring an examination of interstellar light-absorption. This investigation contributes to advancing our current understanding of these celestial objects.

The resolution of distances within our Galaxy enables us to calibrate the distance indicators[43–45]. Open clusters serve as the initial step in the cosmic distance hierarchy and contribute to theories about the early universe. They also provide astronomers with an independent estimation of the size and age of the universe[46,47]. For stars with a known distance (r(pc))and proper motion (μ) in both directions (mas yr^{-1}), one can calculate their tangential velocity (V_t) (km s^{-1}) to the line of sight[48]. On the other hand, the distribution in the Galaxy can be studied by measuring the distances to globular clusters[49,50].

Let us consider our target of open clusters, where all members are at the same distance (r(pc)) and are dispersed (scattered) around a mean absolute magnitude (M_o) following a Gaussian distribution with dispersion (σ). In this scenario, the probability $p(M)dM$ of a member of the celestial set that has an absolute magnitude in the range (M & $M + dM$), representing the frequency distribution function of the absolute magnitudes of the cluster members, takes the following form[51,52]:

$$p(M)dM = \Phi(M) = \frac{1}{\sigma\sqrt{2\pi}} e^{-\frac{(M-M_o)^2}{2\sigma^2}}, -\infty \le M \le \infty \quad \ldots (1)$$

The distance equation can be written as[53]

$$r(pc) = 10^{1+(m_l - M_o - \sigma y - A - [Fe/H])/5} \quad \ldots (2)$$

where (m_l) is the faintest apparent magnitude of the cluster stars, (A) is the magnitude of the interstellar absorption, [Fe/H] is the metallicity, and (y) is the solution of the transcendental equation.

$$\Lambda(y) = y + e^{-y^2/2}\left\{\sqrt{\frac{\pi}{2}}\left[1 + \mathrm{erf}\left(\frac{y}{\sqrt{2}}\right)\right]\right\}^{-1} - \alpha = 0,$$

and

$$\alpha = \frac{m_l - \bar{m}}{\sigma}.$$

where ($\bar{m}$) is the average value of the apparent magnitude.

The distance r(pc) of the observed members that complete down to a fixed limiting magnitude ($\bar{m}$) in the absolute range $M, M + dM$ is written as

$$r(pc) = 10^{1+0.2(\bar{m}-M)}.$$

The distance modulus is then given by $(m - M) = m_l - M_o - \sigma y - A - [Fe/H]$. Increasing [Fe/H] values negatively affect luminosity; hence, the magnitudes and distances will increase. Metallicity must be subtracted if positive and neglected when negative.

If we now measure the average absolute magnitude for these members, we will obtain.

$$\bar{M} = \frac{\int p(M) M r^3 dM}{\int p(M) r^3 dM}$$

$$= \frac{\int \exp\left\{-\frac{(M - M_o)^2}{2\sigma^2} - 0.6M \ln 10\right\} M dM}{\int \exp\left\{-\frac{(M - M_o)^2}{2\sigma^2} - 0.6M \ln 10\right\} dM}$$

$$= M_o - 0.6\sigma^2 \ln 10 = M_o - 1.382\sigma^2.$$

That is,

$$M_o = \bar{M} + 1.382\sigma^2 \quad \ldots (3)$$

Therefore, the last relation between (M_o) and (σ)[54] predicts ($M_o > \bar{M}$); *i.e.*, the stars one sees at a given absolute magnitude are, on average, more luminous than the average for all the stars in each volume. This effect ($i.e., 1.382\,\sigma^2$) is called the Malmquist bias, which arises because, when one selects stars of fixed absolute magnitude, the volume element containing the more distant, intrinsically luminous stars is larger than that occupied by the nearer, fainter objects. The Malmquist bias also plays an important role in connection with counts of radio Galaxies, quasars, and other objects that have been used as cosmological probes.

For the above method of distance computation, Table 2 presents our obtained results devoted to Pis open clusters, arranged as follows:

Table 2 — Our computed distances (r_c(pc)) and the estimated ones (r_e(pc)) by Gaia DR3 with the percentage relative error (ε %).

Clusters	m_l mag	$\bar{m}$ mag	$\bar{M}$ mag	σ	α	r_c pc	r_e pc	ε %
Pis 1	17.997	16.240	2.047	1.278	1.375	6463 ± 80	6897.55	6.31
Pis 2	17.999	16.936	3.644	0.945	1.125	4604 ± 68	4524.89	1.75
Pis 3	17.999	16.825	4.852	1.055	1.113	2378 ± 49	2481.39	4.15
Pis 4	17.931	14.436	5.189	2.341	1.493	725 ± 27	707.21	2.48
Pis 5	17.996	15.753	5.808	2.330	0.963	967 ± 31	974.66	0.78
Pis 7	17.989	16.566	2.446	1.081	1.316	7270 ± 85	6666.66	9.05
Pis 8	17.984	15.709	4.276	1.451	1.568	2119 ± 46	1934.24	9.54
Pis 11	17.773	15.572	3.197	1.545	1.425	3135 ± 56	2985.00	5.03
Pis 12	17.989	15.890	4.062	1.305	1.608	2248 ± 47	2320.20	3.12
Pis 15	17.994	15.964	3.709	1.104	1.839	2770 ± 53	2824.86	1.91
Pis 16	17.587	14.246	2.003	1.350	1.668	3160 ± 56	2808.99	12.49
Pis 17	17.953	14.942	2.759	1.746	1.725	2449 ± 50	2732.24	10.38
Pis 18	17.990	16.086	3.691	1.240	1.535	3242 ± 57	3012.05	7.65
Pis 19	17.999	16.819	3.851	0.878	1.344	3564 ± 60	3921.57	9.13
Pis 20	17.996	15.666	2.986	1.622	1.436	3410 ± 58	3436.43	0.77
Pis 21	17.855	15.789	3.101	1.573	1.313	3250 ± 57	3448.28	5.75
Pis 22	17.973	15.993	1.036	1.333	1.485	10207 ± 101	9803.92	4.11
Pis 23	17.974	17.062	3.162	0.858	1.063	5647 ± 75	6024.10	6.25

Column 1: Cluster name

Columns 2 and 3: Faintest and average values of the apparent magnitudes, respectively

Column 4: Average values of the absolute magnitudes

Column 5: Dispersion

Column 6: Ratio carried out between apparent magnitude and dispersion.

Columns 7 and 8: Our computed distances (r_c(pc)) and those estimated (r_e(pc)) with Gaia DR3, respectively.

Column 9: Percentage relative error (%)

Figure 1 shows a correlation coefficient (∼99%) between our computed distances (r_c(kpc)) as abscissa and those estimated ones (r_e(kpc)) with Gaia as ordinate. Here, it is mentioned slightly that no systematic difference is shown between our findings and Gaia results.

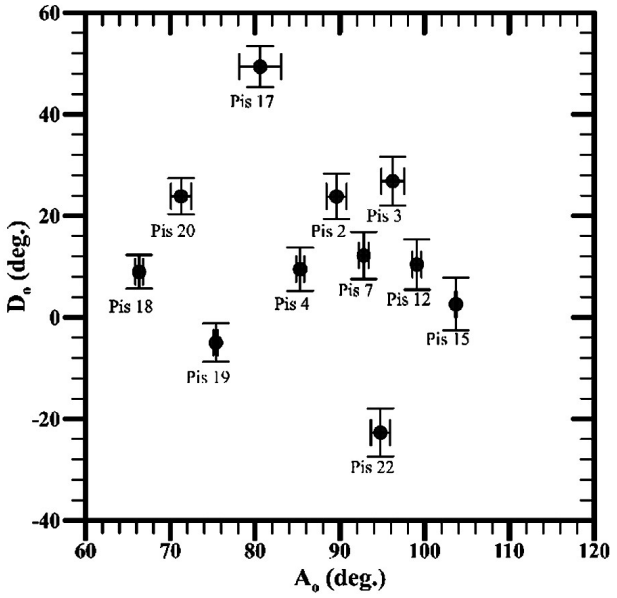

Fig. 1 — Consistency between our computed distances (abscissa; r_c), listed in the seventh column of Table 1, and Gaia distances (ordinate; r_e), presented in the ninth column. Error bars are included, demonstrating a high correlation coefficient of approximately 99%.

3.2 Dynamical Parameters

Unfortunately, for rare studies of our considered objects, we focus on the dynamical processes that occur with rarely studied old and rich ones: Pis 3 (N = 1083)(C 0829-385; OCL 731; MWSC 1498) located in an obscured region[55]. The first analysis of Pis 3 was conducted[56] with CCD BV photometry; and the conclusions indicated a distance of about 1.5 kpc from the Sun, E (B–V) = 1.35 mag, and an age of approximately 2 Gyr with a metallicity (Z = 0.008). On the other hand, Tadross[21] re-investigated and presented a morphological investigation of the 2MASS[22] catalog (Two Micron All Sky Survey) of this rarely studied cluster. The estimation of cluster structure provided limiting and tidal radii of about 2.128 and 12 pc, respectively. Tadross[21] at the same time refined and re-determined the basic photometrical parameters of the Pis3 cluster (e.g., reddening, distance modulus, age, and metal content) by fitting a Padova isochrone to the CMD with Solar metallicity (Z = 0.019) and age 2.24 Gyr. He concluded that its total mass is within 560 $M_\odot$ and the distance is about 2090 ± 95 pc.

In the subsequent analysis, our calculations involve Pis 3's total collective mass (M_C) and hence the average mass ⟨m⟩. Utilizing the well-established mass-luminosity relation (MLR) and isochrones[57] with an age of 2.24 Gyr and metallicity (Z = 0.019), we can derive the mass ratio $\left(M/M_{\odot}\right)$ of each member star as a function of absolute magnitude G using a second-order polynomial.
That is,

$$\frac{M}{M_{\odot}} = 1.749 - 0.117\, M_G - 0.003\, M_G^2. \quad \ldots (4)$$

In the Galactic disk, the effect on the gravitational massive body (*e.g.*, star clusters) is given[58].
That is,

$$x_L = \left[\frac{GM_C}{4A(A-B)}\right]^{1/3} = \left[\frac{GM_C}{4\Omega_o^2-\kappa^2}\right]^{1/3} \quad \ldots (5)$$

where (x_L) is the gap of the Lagrangian points within the center, (M_C) is the sum of the collective mass toward the gap from the center, which is mentioned in the tidal radius (r_t) of the cluster $(i.e., x_L \approx r_t)$, into which the star undergoes equal forces due to gravitational pull toward the cluster and in opposite direction (*i.e.*, the Galactic Center), $(\Omega_o = |A - B|)$is the angular velocity, $\left(\kappa = \sqrt{-4B(A-B)}\right)$ is the epicyclic frequency at the position of the Sun (both in km s^{-1} kpc^{-1}) with a ratio $(\kappa/\Omega_o) = 1.35 \pm 0.05$[59], (A) and (B) are Oort's constants, 15.3 ± 0.4 km s^{-1} kpc^{-1} and −11.9 ± 0.4 km s^{-1} kpc^{-1}, respectively[60], and G = 4.30 × 10^{-6}km $M_{\odot}^{-1}(km\ s^{-1})^2$ is the gravitational constant.

Fukushige and Heggie[61] imply oriented axes and place the mass at the center $(x_\circ, y_\circ, z_\circ)$ of the cluster.This positions the Galactic origin (center) at (-R_{gc}, 0, 0), making the cluster size significantly smaller than R_{gc}. Furthermore, considering a constant angular velocity **ω** = (0, 0, ω) for the cluster, which moves in a circular path around the Galactic Center, the equation of motion for the stars is as follows:

$$\frac{d^2r}{dt^2} = -\nabla\phi_c(r) - 2\omega \times \frac{dr}{dt} + \omega^2(3xe_x - ze_z), \quad \ldots (6)$$

and

$$\omega = \sqrt{\frac{GM_C}{3r_t^3}}. \quad \ldots (7)$$

where (ϕ_C) is the cluster tidal field at position (r), and (e_x, e_z) are unit vectors along (x, z) axes. In such a way, and for Eq. (6), the first term of the right-hand side is devoted to the gravitational acceleration from the cluster, the middle one presents the Coriolis acceleration, while the last term considers both tidal and centrifugal forces.

Also, in their consideration of the time scale model of escape from the cluster as a function of tidal radius (r_t), they found that the energy (E) of the star is just higher than the potential ($E_{crit} = -3GM_C/2r_t$) at the Lagrangian points. These points, also known as the escape radius (r_{esc}), mark where stars are no longer significant in terms of the cluster potential. In this way, the cluster evolution experiences no further inputs. Madrid[62] concluded that the stars are evacuated (ejected) because of where the cluster's center distance is surpassed (r_{esc}) and when the stars have sufficient energy to overcome the external field contribution.

In some N-body calculations[63], the tidal effect is treated as a cutoff, *i.e.*, stars are removed as soon as they cross the tidal radius (r_t), now the timescale for escape (t_{esc}) of phase volume across the tidal boundary, assuming[61] $E - E_{crit} = 0.03\ (km\ s^{-1})^2$

That is,

$$t_{esc} = \frac{\pi r_t}{8(E-E_{crit})}\sqrt{\frac{2GM_C}{r_t}}. \quad \ldots (8)$$

Maciejewski and Niedzielski[64] state that the open cluster reaches Maxwellian stability, equilibrium realizing the forces of contraction and/or destruction with a time called the relaxation time (T_{relax}). During that time, individual stars with low masses possess the largest random velocity (*i.e.*, energies) and occupy a bigger measure in size than the highest masses[65]. Mathematically, (T_{relax}) takes the following form[66]:

$$T_{relax} = \frac{8.9\times10^5\sqrt{N}R_h^{3/2}}{\langle m\rangle^{1/2}\log(0.4N)}. \quad \ldots (9)$$

where R_h (pc) is the radius having about 50% of the mass (*i.e.*, $R_h = 0.5\ r_{lim}$), ⟨m⟩ is the average bulk mass of the cluster stars, and (N) is the members of the cluster star.

Mathieu and Latham[65] defined the time required for the cluster core region to be damped or relaxed as a dynamical crossing time ($T_{cross} = D/\sigma_V$, on the order of10^6 years), where (D) is the cluster diameter, which corresponds to the limiting radius (*i.e.*, D >r_{lim}).

For enough cluster members, the time needed to eject all its members from internal stellar encounters is defined as the evaporation time (τ_{ev})[67], which should be greater than 10^8 years. The evaporation time(τ_{ev})for a stellar system in virial equilibrium is on the order 10^2 (T_{relax}). To ensure the cluster remains bound, the escaping velocity (V_{esc}) resulting from rapid gas removal from the

cluster $\left(V_{esc} = R_{gc}\sqrt{2GM_C/3r_t^3}\right)$[61,68] must be less than the dispersion velocity (σ_V)[69]. Thus, a bound group will emerge only if the starformation efficiency (SFE, which characterizes most cluster-forming dense cores) is greater than 50%[70]. Table 3 presents our dynamical calculations of Pis 3 with 1083 members, a total mass of 1206 ± 35 $M_\odot$, an average mass of 1.113 $M_\odot$, an escaping velocity of 331 ± 5.50 km s^{-1}, a rotational velocity $\left(\omega = \Omega_o R_{gc}\right)$ of 212.48 km s^{-1}, a relaxation time of about 11.56 ± 3.40 Myr, a crossing time of 1.363 ± 0.014 Myr, and an escape time scale (t_{esc}) of about 1.06 × 10^9 yr. The table also provides values from other authors.

3.3 Kinematical Structure

If we imagine our Galaxy to be an axially symmetric system in a steady state in which stars are distributed at random in their orbits, then, from considerations of symmetry alone, we expect to locate one axis of the star's elliptical velocity within the Galactic plane pointing exactly at the Galactic origin[51]. This expectation is confirmed by analysis of velocity ellipsoid parameters (VEPs) with our series of articles, as well as our bold conclusion that the longitude of the vertex (l_2) often differs significantly from zero[75,76].

According to processes taking place in/out with open clusters, in what follows, we focus on some kinematical characteristics devoted to Pismis clusters. Our obtained results are presented in Table 4.

Considering the well-known basic equations governing the position (x, y, z) from the Sun along the equatorial system and the distance r(pc) of the star members[51],

i.e.,

$$x = r\cos\delta\cos\alpha, \quad \ldots (10)$$

$$y = r\cos\delta\sin\alpha, \quad \ldots (11)$$

$$z = r\sin\delta. \quad \ldots (12)$$

Differentiating Eqs. (10, 11, and 11) with respect to time, we obtain stellar velocities (V_x, V_y, V_z) along the (x, y, z) axes concerning the Sun. These velocities include the proper motions along the right ascension $\mu_\alpha \cos\delta$ (mas yr^{-1}), declination μ_δ (mas yr^{-1}), and radial velocity V_r(km s^{-1}).

i.e.

$$V_x = -V_\alpha \sin\alpha - V_\delta \sin\delta\cos\alpha + V_r \cos\delta\cos\alpha,$$
$$V_y = +V_\alpha \cos\alpha - V_\delta \sin\delta\sin\alpha + V_r \cos\delta\sin\alpha,$$
$$V_z = +V_\delta \cos\delta + V_r \sin\delta. \quad \ldots (13)$$

Here,

$$V_\alpha = 4.74 r_i \mu_\alpha \cos\delta,$$
$$V_\delta = 4.74 r_i \mu_\delta,$$

and

$$V_t^2 = V_\alpha^2 + V_\delta^2.$$

where (V_α) and (V_δ) are the components of velocities along with the coordinate system whose center is the cluster's core and (V_t) is the tangential velocity of the cluster.

To obtain the components of space velocities (U, V, W) along with Galactic coordinates as afunction of stellar velocities in space (V_x, V_y, V_z), derived relative to the Sun[77], the transformation from equatorial to Galactic coordinates is performed. This transformation is based on NIR data from 2 MASS[22] and radio observation data.

That is,

Table 3 — Dynamic characteristics of the Pis 3 cluster.

Parameters	Value	Author
Membership (N)	1083	14
	450	21
Total mass $M_C(M_\odot)$	1206 ± 35	Present study
	560	21
Average mass $\langle m\rangle(M_\odot)$	1.113	Present study
Tidal radius r_t (pc)	14.60 ± 1.26	Present study
	12	21
V_{esc} (km s^{-1})	331 ± 5.50	Present study
A (km s^{-1} kpc^{-1})	12.833 ± 1.581	Present study
	19	71, 72
	14.40 ± 1.20	73
	15.30 ± 0.40	60
	15.60 ± 1.60	74
B (km s^{-1} kpc^{-1})	−10.734 ± 1.276	Present study
	−24	71, 72
	−12.0 ± 2.80	73
	−11.90 ± 0.40	60
	−13.90 ± 1.80	74
$\Omega_o = \lvert A - B\rvert$(km s^{-1} kpc^{-1})	23.567	Present study
	33	71, 72
	26.4	73
	27.2	60
	29.50	74
Rotational velocity (ω) (km s^{-1})	212.48	Present study
	247.5	71, 72
	198.50	73
	204	60
	221.20	74
T_{relax} (Myr)	11.56 ± 3.40	Present study
	8.60	21
T_{cross} (Myr)	1.363 ±0.014	Present study
σ_V(km s^{-1})	99.00 ± 1.10 km s^{-1}	Present study
τ_{ev} (Myr)	1156 ± 34.00	Present study
t_{esc} (yr)	1.06 × 10^9	Present study

Table 4 — Kinematical structure; the apex position (A_o, D_o), dispersion velocities (σ_j), the longitude of the vertex (l_2), and Solar elements of Pismis's clusters.

Clusters	A_o, D_o deg.	$\sigma_1, \sigma_2, \sigma_3$ km s^{-1}	l_2 deg.	$X_\odot, Y_\odot, Z_\odot$, R_{gc} kpc	Authors	Solar elements $S_\odot$, l_A, b_A	Space Velocity km s^{-1}	Age[e] Gyr
Pis 2	89.610, 23.794	499.019, 54.358, 14.160	–0.147146	–0.888, –4.510, –0.268, 10.150	Present study	201.658, –5.945, 0.317	201.658	1.148
	-	-	-	–0.772, –3.920, –0.233, 9.919	14	-	147.702[c]	-
Pis 3	96.247, 26.823	98.876, 5.986, 2.013	–0.096241	–0.511, –2.323, 0.021, 9.016	Present study	97.168, –6.081, –6.402	97.168	1.072
	-	-	-	–0.487, –2.264, 0.020, 9.113	14	-	95.027[c]	-
Pis 4	85.327, 9.475	29.134, 0.767, 0.487	–0.225077	–0.089, –0.719, –0.030, 8.321	Present study	29.235, –16.424, 10.963	29.236	0.034
	-	-	-	–0.085, –0.687, –0.028, 8.453	14	-	34.249[c]	-
Pis 7	92.815, 12.168	252.806, 60.937, 5.440	–0.015766	–1.380, –7.133, 0.253, 11.947	Present study	157.031, –17.613, 3.221	157.032	0.501
	-	-	-	–1.057, –5.467, 194.1, 10.871	14	-	136.483[c]	-
Pis 12	99.104, 10.388	82.158, 4.176, 1.386	–0.369807	–0.053, –2.244, 0.126, 8.553	Present study	81.769, –22.023, –1.446	81.769	2.512
	-	-	-	–0.051, –2.170, 0.122, 8.667	14	-	91.463[c]	-
Pis 15	103.709, 2.566	76.208, 5.339, 1.531	–0.508996	0.121, –2.765, 0.139, 8.541	Present study	75.815, –31.067, –2.048	75.816	1.288
	-	-	-	0.114, –2.605, 0.130, 8.629	14	-	85.556[c]	-
Pis 17	80.609, 49.340	70.607, 2.821, 1.125	–0.307460	0.819, –2.308, 0.005, 7.734	Present study	71.222, 19.635, –6.835	71.222	0.010
	-	-	-	0.848, –2.339, 0.048, 7.864	14	-	29.919[f]	-
Pis 18	66.318, 8.954	59.912, 5.353, 1.361	–0.275590	2.007, –2.547, 0.018, 6.697	Present study	59.192, –6.177, 27.065	59.192	1.202
	-	-	-	1.713, –2.175, 0.015, 6.975	14	-	85.00[c]	-
Pis 19	75.389, –4.974	278.905, 28.816, 7.517	–0.758570	2.508, –2.533, –0.019, 6.231	Present study	96.041, –24.797, 26.601	96.041	0.794
	-	-	-	2.474, –2.499, –0.019, 6.376	14	-	109.93[c]	-
Pis 20	71.273, 23.851	98.425, 13.065, 2.350	–0.053985	2.631, –2.168, –0.072, 5.976	Present study	98.184, 3.447, 14.269	98.184	0.007
	-	-	-	2.413, –1.988, –0.066, 6.252	14	-	104.750[c]	-
Pis 22	94.798, –22.697	1122.970, 50.644, 31.170	–0.875263	8.967, –4.874, –0.108, 4.935	Present study	286.662, –50.453, 16.595	286.662	0.040
	-	-	-	6.722, –3.654, –0.080, 3.996	14	-	215.625[c]	-

(c) [17], (e) [22], and (f) [89]

$$U = -0.0518807421\ V_x - 0.872222642\ V_y - 0.4863497200\ V_z,$$
$$V = +0.4846922369\ V_x - 0.4477920852\ V_y + 0.5713692061 V_z,$$
$$W = -0.8731447899\ V_x - 0.1967483417\ V_y + 0.4459913295\ V_z. \quad \ldots (14)$$

- **The Apex of the Moving Cluster**

Virtually, star members appear as coherent and associated with moving open clusters sharing similar properties, such as distance, kinematics, chemical composition, and age, as well as the radial velocity (V_r). Thedetermination of the point (A_o, D_o) by which the action of the stars in the cluster will merge (i.e., apex) is one of the main important tasks in the kinematical and physical examination[78–81]. For this purpose, there are numerous techniques, such asi) the

classical convergent point method, ii) the AD chart method, and iii) the convergent point search method (CPSM[82]).

In our current work, we focus on the AD chart method (stellar apex method), which is based on the distribution of individual apexes with members in the equatorial coordinate system. This procedure was known and developed[83,84] and has been frequently used[85,86] in the direction of determining apexes and other numerous kinematical parameters, as well as their central kinematical substructures (*e.g.*, M67, NGC 188, Pleiades, Castro & UMa, and IC 2391). In this manner,

$$A_o = tan^{-1}\left(\frac{\overline{V_y}}{\overline{V_x}}\right), \quad \text{... (15)}$$

$$D_o = tan^{-1}\left(\frac{\overline{V_z}}{\sqrt{\overline{V_x}^2+\overline{V_y}^2}}\right). \quad \text{... (16)}$$

Returning to Table 1, which presents the radial velocities of only 11 Pismis clusters[17] and considering the two above equations, Fig. 2 shows the apex position (A_o, D_o) of these clusters with an AD chart method with comments.

- **The Direction Cosines (l_j, m_j, n_j)**

The direction cosines $l_j, m_j, \text{and } n_j (\forall j = 1,2,3)$ are associated with the eigen value problem $(\lambda_j; \forall j = 1,2,3)$, matrix elements (μ_{ij}), and dispersion velocities $(\sigma_j; \forall j = 1,2,3)$ along three axes[75]. Mathematically, this is expressed as follows:

$$l_j = [\mu_{22}\mu_{33} - \sigma_j^2(\mu_{22} + \mu_{33} - \sigma_j^2) - \mu_{23}^2]/D_j,$$
$$m_j = [\mu_{23}\mu_{13} - \mu_{12}\mu_{33} + \sigma_j^2\mu_{12}]/D_j,$$
$$n_j = [\mu_{12}\mu_{23} - \mu_{13}\mu_{22} + \sigma_j^2\mu_{13}]/D_j, \quad \text{... (17)}$$

where $(l_j^2 + m_j^2 + n_j^2 = 1)$ is an initial test for our code for our sample and

$$D_j^2 = (\mu_{22}\mu_{33} - \mu_{23}^2)^2 + (\mu_{23}\mu_{13} - \mu_{12}\mu_{33})^2 + (\mu_{12}\mu_{23} - \mu_{13}\mu_{22})^2 + 2[(\mu_{22} + \mu_{33})(\mu_{23}^2 + \mu_{22}\mu_{33}) + \mu_{12}(\mu_{23}\mu_{13} - \mu_{12}\mu_{33}) + \mu_{13}(\mu_{12}\mu_{23} - \mu_{13}\mu_{22})]\sigma_j^2 + (\mu_{33}^2 + 4\mu_{22}\mu_{33} + \mu_{22}^2 - 2\mu_{23}^2 + \mu_{12}^2 + \mu_{13}^2)\sigma_j^4 - 2(\mu_{22} + \mu_{33})\sigma_j^6 + \sigma_j^8.$$

The analysis can be simplified by exploiting the empirical fact that one axis of the velocity ellipsoid is always found to be arranged perpendicular to the Galactic plane so that the other two axes must lie in the plane. It is also found empirically that the longest axis of the ellipsoid (i.e., the direction of maximum velocity dispersion) points approximately in the way of the Galactic Center. Therefore, to specify the orientation of the velocity ellipsoid, we need to determine only the Galactic longitude along which the principal axis lies. This longitude is called the longitude of the vertex (l_2).

Table 4 reveals discrepancies in our Pismis results concerning l_2. We observe that these values do not align within a specific range. Additionally, we highlight that the longitude of the vertex (l_2) is very small for those old ages (~Gyr), as shown in Fig. 3.

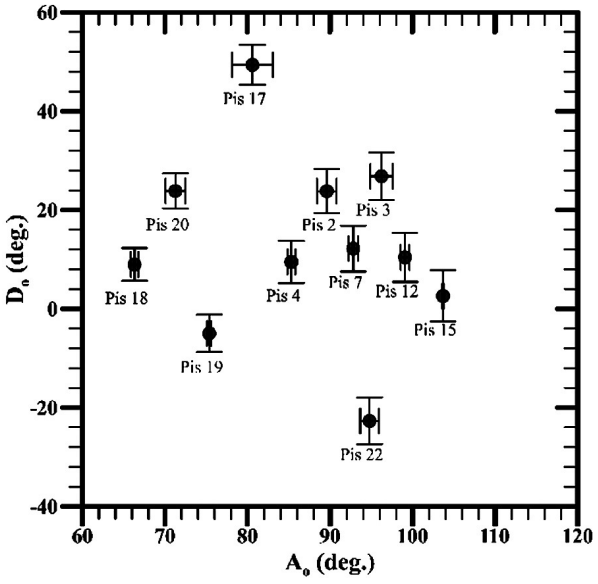

Fig. 2 — The (A_o, D_o) apex position for 11 Pismis clusters with error bars.

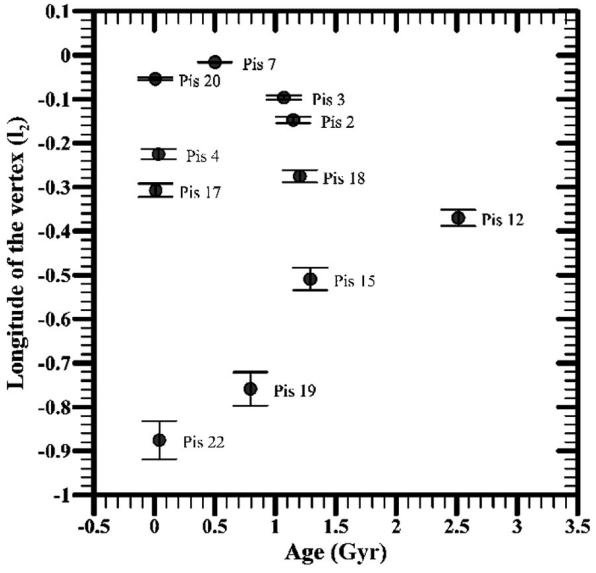

Fig. 3 — Variation of longitude of the vertex (l_2) *vs.* age (Gyr) with error bars of the Pismis clusters under investigation.

This discrepancy may be attributed to formation mechanisms influenced by various physical conditions, including factors such as metallicity and opacity.

- **Projected Distances**

Considering our calculated distances (r_c) with the overlaid markers, we proceed to include these distances in relation to the Galactic Center $\left(R_{gc}\right)$[51]. This involves expressing them as a function of the Sun's distance from the Galactic Center ($i.e., R_o = 8.20 \pm 0.10$ kpc)[84], *i.e.*, $R_{gc}^2 = R_o^2 + r_c^2 - 2R_o r_c \cos l$. This allows us to compute the anticipated (projected) distances toward the Galactic plane $(X_\odot, Y_\odot)$, and the distance from the Galactic plane $(Z_\odot)$[85] may be computed as follows:

$$X_\odot = r_c \cos b \cos l,$$
$$Y_\odot = r_c \cos b \sin l,$$
$$Z_\odot = r_c \sin b. \quad \ldots (18)$$

- **Solar motion**

Solar motion can be characterized as the absolute value of the Sun's velocity relative to our streams under consideration,
i.e.,

$$S_\odot = \sqrt{\bar{U}^2 + \bar{V}^2 + \bar{W}^2}. \quad \ldots (19)$$

Moreover, the Galactic longitude $(l_A)$and Galactic latitude (b_A) of the Solar apex are calculated as follows:

$$l_A = \tan^{-1}\left(\frac{-\bar{V}}{\bar{U}}\right), \quad \ldots (20)$$

$$b_A = \sin^{-1}\left(\frac{-\bar{W}}{S_\odot}\right). \quad \ldots (21)$$

4 Conclusion

Our present work focused on the following key points:

i) Using the distance equation, we computed distances (r_c(pc)) for seldom-studied and aged southern Milky Way Pismis's open clusters. This computation assumed that all members are distributed around magnitude (M_o) with dispersion (σ). We compared our obtained results (r_c(pc)) with the estimated distances(r_e(pc))from the Gaia database, revealing a high correlation coefficient of approximately 99%.

ii) With a particular focus on Pismis 3, a rarely studied and old cluster with significant richness (i.e., N = 1083), we computed its dynamics, total mass, and evolutionary times based on both limiting and tidal radii. These results were then compared with findings from other authors, as summarized in Table 3.

iii) Specifically for 11 aged clusters with available radial velocities, we conducted a kinematical analysis. This involved determining the apexes (A_o, D_o)using the AD chart method, velocity ellipsoid parameters (VEPs), and the Galactic longitude of the vertex (l_2)in conjunction with their respective ages (Myr).

Acknowledgments

The authors are deeply thankful to the referee for his/her valuable and constructive comments that improved the original manuscript.

This investigation has made use of the VizieR catalog gate tool, CDS, Strasbourg, France. The reparation of this work has made the extensive operation of NASA's Astrophysics Data System Bibliographic Services. This work presents results from the European Space Agency (ESA) space mission Gaia. Gaia data are being processed by the Gaia Data Processing and Analysis Consortium (DPAC). Funding for the DPAC is provided by national institutions, in particular the institutions participating in the Gaia Multi-Lateral Agreement (MLA). The Gaia mission website is https://www.cosmos.esa.int/gaia. The Gaia archive website is https://archives.esac.esa.int/gaia. The authors extend their appreciation to the Deanship of Research and Graduate Studies at University of Tabuk for funding this work through Research No. 0137-1444-S.

References

1 Trumpler R J, *Lick Obs Bull*, 14 (1930) 154.
2 Moffat A F J & Vogt N, *Astron Astrophys*, 23 (1973) 317.
3 Janes K & Adler D, *Astrohys J Supp Ser*, 49 (1982) 425.
4 Friel E D, *Ann Rev Astron Astrophys*, 33 (1995) 381.
5 Moitinho A, Star clusters: Basic galactic building blocks throughout time and space, Edt by Grijs R de & Lépine J R D, *IAU Symp*, 266 (2010) 106.
6 Moraux E, *EAS Publ Ser*, 80 (2016) 73.
7 Vandenberg D A, *Astrohys J Supp Ser*, 51 (1983) 29.
8 Barnes S A, *Astrophys J*, 669 (2007) 1167.
9 Salaris M, Asteroseismology of stellar populations in the milky way, Springer International Publishing, Switzerland, (2013) 9.
10 Bertelli M C, Salaris M, Pasquali A & Grebel E K, *Month Not Royal Astron Soc*, 466 (2017) 2161.
11 Marino A F, Milone A P, Casagrande L, *et al.*, *Astrophys J*, 863 (2018) L33.
12 Pismis P, *Bol Obs Tonantzintla Tacubaya*, 18 (1959) 39.
13 Dias W S, Alessi B S, Moitinho A, *et al.*, *Astron Astrophys*, 389 (2002) 871.
14 Gaia Collaboration 2022, *VizieR Online Data Catalog*, 1355 (2022) I/355.
15 Weiler M, *Astron Astrophys*, 617 (2018) A138.
16 Fürnkranz V, Meingast S & Alves J, *Astron Astrophys*, 624 (2019) A11.

17 Soubiran C, Cantat-Gaudin T, *et al.*, *Astron Astrophys*, 619A (2018) 155.
18 Lindoff U, *ArkivAstron*, 5 (1968) 63.
19 Di F L, Bragaglia A, Tosi M & Marconi G, *Month Not Royal Astron Soc*, 328 (2001) 795.
20 Dutra C M & Bica E, *Astron Astrophys*, 359 (2000) 347.
21 Tadross A L, *Ch J Astron Astrophys*, 8 (2008) 362.
22 Skrutskie M F, Cutri R M, Stiening R, *et al.*, *Astron J*, 131 (2006) 1163.
23 Sampedro L, Dias W S, Alfaro E J, Monteiro H & Molino A, *Month Not Royal Astron Soc*, 470 (2017) 3937.
24 Bonatto C & Bica E, *Month Not Royal Astron Soc*, 397 (2009) 1915.
25 Lynga G, Lund catalogue of open cluster data (Centre de Donn´eesStellaires, Strasbourg), 5th Edn, 1987.
26 Ahumada J A, *Astron Nachr*, 326 (2005) 3.
27 Giorgi E E, Baume G, Solivella G & Vázquez R A, *Astron Astrophys*, 432 (2005) 491.
28 Marco A & Negueruela I, *Astron Astrophys*, 493 (2009) 79.
29 Moffat A F J &Vogt N, *Astron Astrophys Supp Ser*, 20 (1975) 85.
30 Reyle C & Robin A C, *Astron Astrophys*, 384 (2002) 403.
31 Carraro G, Geister D, Baume G, Vázquez R & Moitinho A, *Month Not Royal Astron Soc*, 360 (2005) 655.
32 Rastorguev A S, Glushkova E V, Dambis A K & Zabolotskikh M V, *PAZh*, 25 (1999) 689.
33 Hatzidimitriou D, Held E V, *et al.*, *Astron Astrophys*, 626 (2019) 90.
34 Carraro G & Munari U, *Month Not Royal Astron Soc*, 347 (2004) 625.
35 Orsatti A M, Vega E I & Marraco H G, *Astron Astrophys*, 408 (2003) 135.
36 Piatti A E, Clari´a J J & Bica E, *Astron Astrophys*, 360 (2000) 529.
37 Ilovaisky A S & Lequeux J, *Astron Astrophys*, 18 (1972) 169.
38 van den Bergh S, *Astroph J Supp*,38 (1978) 119.
39 Lynga G, *Medd Fran Lunds Observatorium Ser II*, 143 (1965).
40 van den Bergh S & Hagen G L, *Astron J*, 80 (1975) 11.
41 Lauberts A, The ESO/Uppsala survey of the ESO (B) atlas, (ESO,Garching, Germany), 1982.
42 Claria J J& Piatti A E, *Astrophys Space Sci*, 290 (2004) 353.
43 Shanks T, *Month Not Royal Astron Soc*, 290 (1997) 77.
44 Tanvir N R, Cepheids as distance indicators, *Conf in Space Telescope Science Institute Series*, Theextra-galactic distance scale, Edt by Livio M, Cambridge University Press, (1997) 91.
45 Borchkhadze T M & Kogoshvili N G, *Astrophysics*, 42 (1999) 25.
46 Willick J A & Batra P, *Astrophys J*, 548 (2001) 564.
47 Mazumdar A & Narasimha D, *Bull Astro Soc India*, 27 (1999) 267.
48 Robinson R M, The cosmological distance ladder, (Freeman, New York), 1985.
49 Cassisi S, De Santis R & Piersimoni A M, *Month Not Royal Astron Soc*, 326 (2001) 342.
50 Duncan D, Chaboyer B, Carney B, Girard T, Latham D, Layden A, McWilliam A, Sarajedini A & Shao M, *Bull Am Astron Soc*, 33 (2001) 881.
51 Mihalas D & Binney J, Galactic astronomy (Freeman, New York), 1981.
52 Scheffler H & Elsasser H, Physics of the galaxy and interstellar matter, (Springer-Verlag, Berlin), 1988.
53 Abdel-Rahman H I, Issa I A, Sharaf M A, Nouh M I, Bakry A, Osman A I, Saad A S, Kamal F Y & Essam, *J Korean Astron Soc*, 42 (2009) 71.
54 Bok B J, The distribution of stars in space, (Chicago University Press, Chicago), 1937.
55 Janes K A, In calibration of stellar ages, Davis L Press, Schenectady, (1988) 59.
56 Carraro G & Ortolani S, *Astron Astrophys*, 291 (1994) 106.
57 Marigo P, *et al.*, *Astrophys J*, 835 (2017) 77.
58 Röser S & Schilbach E, *Astron Astrophys*, 627 (2019) A4.
59 Binney J & Merrifield M, Galactic astronomy, Princeton series in astrophysics (Princeton University Press), 1998.
60 Bovy J, *Month Not Royal Astron Soc*, 468 (2017) L63.
61 Fukushige T & Heggie D C, *Monty Not Royal Astron Soc*, 318 (2000) 753.
62 Madrid J P, Hurley J R & Sippel A C, *Astrophys J*, 756 (2012) 167.
63 Portegies Z S F, Hut P, Makino J & McMillan S L W, *Astron Astrophys*, 337 (1998) 363.
64 Maciejewski G & Niedzielski A, *Astron Astrophys*, 467 (2007) 1065.
65 Mathieu R D & Latham D W, *Astron J*, 92 (1986) 1364.
66 Spitzer L & Hart M H, *Astrophys J*, 166 (1971) 483.
67 Adams F C & Myers P, *Astrophys J*, 533 (2001) 744.
68 Fich M & Tremaine S, *Ann Rev Astron Astrophys*, 29 (1991) 409.
69 Lada C J & Lada E A, *Ann Rev Astron Astrophys*, 41 (2003) 57.
70 Wiliing M & Lada C J, *Astrophys J*, 274 (1983) A138.
71 Oort J H, *Bull Astron Inst Netherl*, 3 (1927) 275.
72 Oort J H, *Bull Astron Inst Netherl*, 4 (1927) 91.
73 Kerr F J & Lynden-Bell D, *Mon Not Roy Astron Soc*, 221 (1986) 1023.
74 Nouh M I & Elsanhoury W H, *Astrophysics*, 63 (2020) 179.
75 Elsanhoury W H, Nouh M I & Abdel-Rahman H H, *Rev Mex Astron Astrofis*, 51 (2015) 197.
76 Elsanhoury W H, *Astrophys*, 59 (2016) 246.
77 Liu J C, Zhu Z & Hu B, *Astron Astrophys*, 536 (2011) A102.
78 Wayman P A, Symms L S &Blackwell K C, *R Obs Bull*, 98 (1965).
79 Hanson R B, *Astron J*, 80 (1975) 379.
80 Eggen O J, *Astron J*, 89 (1984) 1350.
81 Gunn J E, Griffin R F, Griffin R F M & Zimmerman B A, *Astron J*, 97 (1998) 198.
82 Galli P A B, Teixeira R, Ducourant C, Bertout C & Benevides-Soares P, *Astron Astrophys*, 538 (2012) 23.
83 Chupina N V, Reva V G & Vereshchagin S V, *Astron Astrophys*, 371 (2001) 115.
84 Chupina N V, Reva V G & Vereshchagin S V, *Astron Astrophys*, 451 (2006) 909.
85 Vereshchagin S V, Chupina N V, Sariya Devesh P, Yadav R K S & Kumar B, *New Astron*, 31 (2014) 43.
86 Postnikova E S, Elsanhoury W H, Sariya Devesh P, Chupina N V, Vereshchagin S V & Jiang I G, *Res Astron Astrophys*, 20 (2020) 16.
87 Bland-Hawthorn J, Sharma S, *et al.*, *Month Not Royal Astron Soc*, 486 (2019) 1167.
88 Tadross A L, *J Korean Astron Soc*, 44 (2011) 1.
89 Conrad C, Scholz R D, *et al.*, *Astron Astrophys*, 600 (2017) A106.